

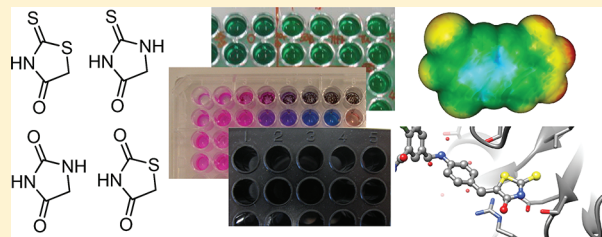
Privileged Scaffolds or Promiscuous Binders: A Comparative Study on Rhodanines and Related Heterocycles in Medicinal Chemistry

Thomas Mendgen, Christian Steuer, and Christian D. Klein*

Medicinal Chemistry, Institute of Pharmacy and Molecular Biotechnology IPMB, Heidelberg University, Im Neuenheimer Feld 364, D-69120 Heidelberg, Germany

S Supporting Information

ABSTRACT: Rhodanines and related five-membered heterocycles with multiple heteroatoms have recently gained a reputation of being unselective compounds that appear as “frequent hitters” in screening campaigns and therefore have little value in drug discovery. However, this judgment appears to be based mostly on anecdotal evidence. Having identified various rhodanines and related compounds in screening campaigns, we decided to perform a systematic study on their promiscuity. An amount of 163 rhodanines, hydantoin, thiohydantoin, and thiazolidinediones were synthesized and tested against several targets. The compounds were also characterized with respect to aggregation and electrophilic reactivity, and the binding modes of rhodanines and related compounds in published X-ray cocrystal structures were analyzed. The results indicate that the exocyclic, double bonded sulfur atom in rhodanines and thiohydantoin, in addition to other structural features, offers a particularly high density of interaction sites for polar interactions and hydrogen bonds. This causes a promiscuous behavior at concentrations in the “screening range” but should not be regarded as a general knockout criterion that excludes such screening hits from further development. It is suggested that special criteria for target affinity and selectivity are applied to these classes of compounds and that their exceptional and potentially valuable biomolecular binding properties are consequently exploited in a useful way.



INTRODUCTION

The five-membered multiheterocyclic (FMMH) rings shown in Figure 1 and in particular the rhodanine scaffold are currently

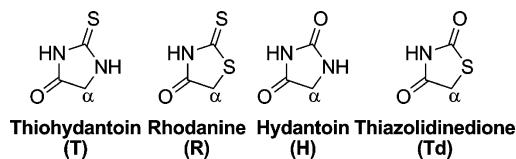


Figure 1. Five-membered multiheterocyclic (FMMH) rings studied in this work with their respective abbreviations given in parentheses.

the object of a controversial debate in the medicinal chemistry community. Whereas some authors¹ characterize them as “frequent hitters” or assay-interfering compounds that broadly interact with a plethora of targets and are therefore practically useless in drug discovery, others² propose to employ these moieties as “privileged scaffolds”. To some extent, these two opinions are two perspectives on a single property, namely, the ability to form interactions with a variety of biological targets. The negative perspective highlights insufficient selectivity, whereas a more positive perspective may be based on the consideration that FMMH derivatives allow a quick identification of “hits” with sufficient target affinity whose selectivity can be tuned in subsequent development steps. The positive perspective may also be linked to a polypharmacological approach in drug discovery, where the affinity toward various targets is regarded as an advantage. In certain cases, such as the inhibition of bacterial

peptidoglycan biosynthesis, the interaction with several targets in a single biosynthetic pathway is in fact highly advantageous.³

The increasing relevance of this class of compounds, at least in the “publication domain” of medicinal chemistry, is highlighted by the fact that we counted 40 publications dealing with FMMH derivatives that appeared in four leading medicinal chemistry journals (*J. Med. Chem.*, *Eur. J. Med. Chem.*, *ChemMedChem*, and *Bioorg. Med. Chem.*) within 1 year (September 2009 to August 2010). In contrast to this, the selectivity issue of FMMHs is primarily discussed in an informal way, and we are not aware of a systematic study that aims at the elucidation of the underlying molecular recognition modes of these compounds, which are responsible for their exceptional binding behavior.

Our own interest in the FMMH scaffolds was piqued when we noticed the similarity between them and some of the scaffolds that we currently pursue in the context of various projects (cf. Figure 2). In fact, a number of these compounds turned out to be active in some of the enzyme assays performed in our group, such as the antibacterial target MurA⁴ or the Dengue virus protease.⁵ In light of the potentially problematic, promiscuous behavior of these compound classes and because of the ongoing discussion, we decided to perform a systematic SAR study of a large array of substituted rhodanines, thiohydantoin, hydantoin, and thiazolidinediones. The initial intent was to screen a large array of compounds against a number of enzymatic

Received: September 19, 2011

Published: November 14, 2011

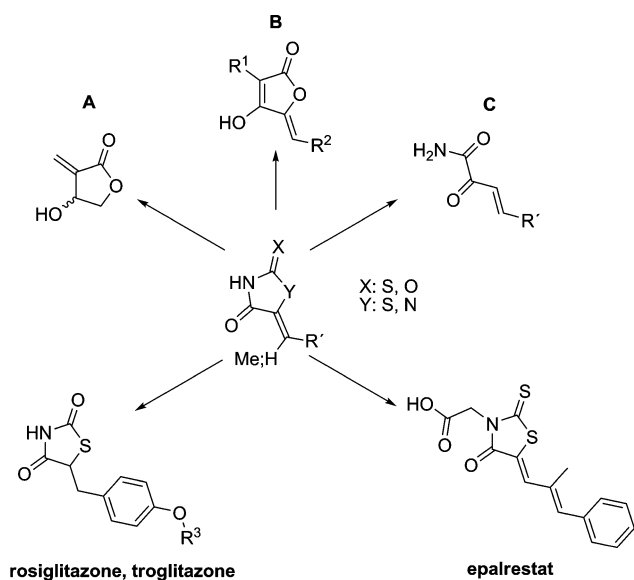


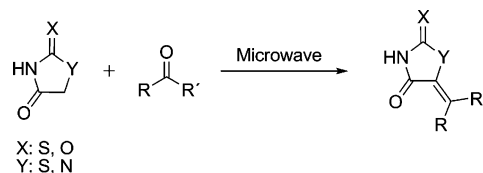
Figure 2. Relationship of the FMMHs to scaffolds that we pursue in other projects (A, B, C) and to drugs from clinical practice: (A) tulipaline derivatives⁷ as MurA inhibitors; (B) tetronic acids as inhibitors of MurA and other enzymes of the peptidoglycan biosynthesis; (C) ketoamides as inhibitors of viral serine proteases.⁸

targets from various classes for which highly reproducible and robust assays have been established in our laboratory. The enzymes included a bacterial transferase (MurA), two serine proteases (thrombin and the protease of Dengue virus), and a metalloprotease (methionine aminopeptidase from *E. coli*, MetAP). This diverse collection of enzymes provides a broad spectrum of chemical and geometrical recognition features for small molecules and therefore allows the identification of truly promiscuous binders, irrespective of the underlying molecular explanation for their promiscuity. We then proceeded to use a number of additional physical, analytical, and theoretical tools to further understand the reason for the exceptional biomolecular binding properties of this class of compounds. For example, compounds from the array that showed a broad inhibition profile were studied by dynamic light scattering (DLS) to identify a possible aggregation-based mode of action.⁶ The binding modes of published cocrystal structures of FMMH derivatives were analyzed, and DFT calculations were performed to study the electronic properties of these compound classes. The results may be helpful in the further discussion on the relevance of rhodanines and related FMMHs in medicinal chemistry.

RESULTS AND DISCUSSION

Chemistry. The synthesis of FMMHs with exocyclic double bond and aromatic heterocycle usually involves a Knoevenagel condensation between the heterocycle and aldehyde or ketone (Scheme 1).^{9–16} Microwave heating was employed (20 min) to shorten the reaction times in comparison to conventional heating. The method of choice included irradiation times of 7–20 min at 160–200 °C, depending on the heterocycle, with a solvent mixture of toluene/ NH_4OAc for the rhodanine (**R**) and thiazolidinedione (**Td**) and acetic acid/ NH_4OAc for the thiohydantoin (**T**) and hydantoin (**H**) compounds. The choice of solvent leads to a selective precipitation of the product, which facilitated the final purification step. Following this procedure, a series of compounds bearing the four different five-membered heterocycles was synthesized.

Scheme 1. Synthesis of Compounds 1–44^a

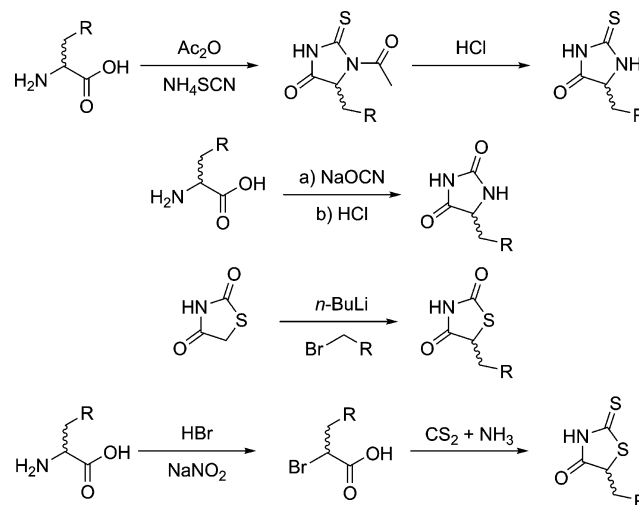


^aA total of 125 derivatives with various elements in the X and Y positions were prepared. The numeric part of the compound identification indicates the nature of R and R', whereas the heterocycle is identified by a letter code (cf. Figure 1). For example, compound **7Td** is a nitrobenzylidene-substituted thiazolidinedione.

In theory, *E* and *Z* isomers can be obtained by this reaction. The preferred product has been reported to have the *Z* geometry.^{17,18} We determined the *E/Z* ratio of the products by HPLC and found all compounds to be single isomers. The expected *Z*-geometry was confirmed by the crystal structure of a representative analogue (**20H**, small-angle X-ray diffraction).

Compounds without exocyclic double bond (no aromatic heterocycle) were synthesized according to standard protocols (Scheme 2). Thiohydantoin and hydantoin were synthesized

Scheme 2. Synthesis of Compounds 45–60



directly from commercially available amino acids with ammonium thiocyanate (**T**) or sodium cyanate (**H**). Subsequent deprotection with concentrated hydrochloric acid furnished the desired compounds.^{19–22} Thiazolidinediones were prepared from the unsubstituted congener by deprotonation with *n*-BuLi followed by a nucleophilic substitution.²³ For the rhodanines, amino acids were first converted into α -halogen carboxylic acids and afterward treated with freshly prepared dithiocarbamate to achieve the ring closure.^{24–26}

Structure–Activity Relationships. The inhibitory activity of the 163 compounds against four different enzymatic targets was determined: the NS2B-NS3 protease of Dengue virus (serine protease),⁵ thrombin from bovine plasma (Thr), a bacterial transferase (*E. coli* MurA),^{4,27} and a metalloprotease (*E. coli* MetAP).²⁸ The concentrations of inhibitors and enzymes were identical to those that we employ in the routine screening procedures. The results of the enzymatic assays are summarized in Table 1 (compounds with aromatic heterocycle) and Table 2 (nonaromatic compounds).

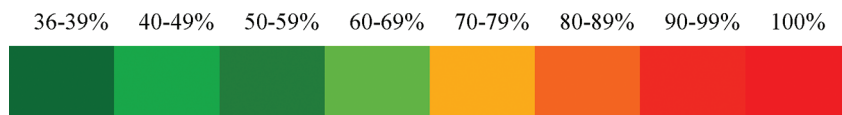
Table 1. Inhibition of Four Enzymatic Targets by 140 Thiohydantoin (T), Rhodanine (R), Hydantoin (H), and Thiazolidinedione (Td) Derivatives^a

	Substituent		NS2B-NS3	Thr	<i>E. coli</i> MurA	<i>E. coli</i> MetAP		Substituent		NS2B-NS3	Thr	<i>E. coli</i> MurA	<i>E. coli</i> MetAP	
1		T	35	17	n.i.	12	2		T	n.i.	21	24	14	
		R	34	31	10	30			R	23	19	33	n.i.	
		H	38	n.i.	100	17			H	n.i.	n.i.	n.i.	n.i.	
		Td	25	15	n.i.	n.i.			Td	30	20	n.i.	12	
3		T	46	27	32	15	4		T	33	10	n.i.	15	
		R	56	28	15	14			R	42	23	n.i.	n.i.	
		H	36	n.i.	n.i.	46			H	n.i.	n.i.	n.i.	n.i.	
		Td	n.i.	19	n.i.	n.i.			Td	30	20	n.i.	12	
5		T	41	20	22	15	6		T	24	29	17	13	
		R	46	23	15	n.i.			n.i.	R	27	25	n.i.	n.i.
		H	15	n.i.	n.i.	n.i.			n.i.	H	14	18	18	n.i.
		Td	13	28	n.i.	n.i.			Td	12	n.i.	n.i.	n.i.	
7		T	35	19	15	13	8		T	42	25	51	75	
		R	46	25	65	11			R	36	21	15	n.i.	
		H	26	n.i.	n.i.	n.i.			H	29	16	n.i.	n.i.	
		Td	n.i.	n.i.	n.i.	13			Td	20	11	n.i.	13	
9		T	31	14	n.i.	15	10		T	55	22	77	n.i.	
		R	41	23	n.i.	n.i.			R	44	26	n.i.	n.i.	
		H	n.i.	n.i.	n.i.	11			H	36	15	n.i.	n.i.	
		Td	17	18	n.i.	n.i.			Td	26	23	n.i.	10	
11		T	43	11	13	15	12		T	50	22	16	n.i.	
		R	48	31	18	n.i.			R	45	27	18	12	
		H	n.i.	n.i.	n.i.	n.i.			H	34	20	n.i.	n.i.	
		Td	11	n.i.	n.i.	n.i.			Td	41	25	n.i.	n.i.	
13		T	50	13	n.i.	n.i.	14		T	48	39	11	n.i.	
		R	42	16	n.i.	n.i.			R	47	34	24	n.i.	
		H	24	10	n.i.	10			H	26	14	n.i.	n.i.	
		Td	19	32	84	11			Td	32	34	n.i.	n.i.	
15		T	28	15	10	18	16		T	28	12	21	15	
		R	33	11	10	n.i.			n.i.	R	29	15	58	12
		H	18	n.i.	n.i.	n.i.			n.i.	H	27	12	n.i.	n.i.
		Td	17	11	25	10			Td	18	n.i.	n.i.	11	
17		T	44	20	18	11	18		T	36	23	46	86	
		R	50	29	n.i.	n.i.			R	50	35	89	65	
		H	18	n.i.	n.i.	n.i.			H	37	32	70	100	
		Td	16	23	n.i.	13			Td	44	37	78	90	
19		T	38	23	72	26	20		T	28	15	10	18	
		R	42	32	66	12			R	33	11	10	n.i.	
		H	13	n.i.	17	n.i.			H	18	n.i.	n.i.	n.i.	
		Td	19	27	100	n.i.			Td	17	11	25	10	
21		T	48	16	n.i.	n.i.	22		T	46	14	22	n.i.	
		R	44	18	n.i.	n.i.			R	52	25	17	n.i.	
		H	16	22	n.i.	n.i.			H	25	23	10	n.i.	
		Td	11	24	30	11			Td	20	19	41	n.i.	
23		T	44	11	31	n.i.	24		T	46	19	19	n.i.	
		R	60	24	20	n.i.			R	47	28	43	n.i.	
		H	13	16	n.i.	n.i.			H	n.i.	n.i.	n.i.	n.i.	
		Td	n.i.	18	44	n.i.			Td	23	11	12	n.i.	
25		T	46	17	75	10	26		T	42	29	22	n.i.	
		R	50	22	21	n.i.			R	54	27	13	n.i.	
		H	22	22	n.i.	n.i.			H	16	25	38	n.i.	
		Td	n.i.	19	62	12			Td	11	29	38	n.i.	
27		T	42	15	57	11	28		T	43	20	50	42	
		R	47	21	18	n.i.			R	45	17	11	n.i.	
29		T	47	38	13	95	30		T	43	18	43	28	
		R	31	n.i.	10	12			R	44	18	n.i.	n.i.	
		Td	15	29	n.i.	12			Td	35	n.i.	n.i.	11	
31		T	29	30	57	83	32		T	37	11	n.i.	n.i.	
		R	53	31	18	18			R	42	24	24	n.i.	
33		T	n.i.	14	77	19	34		T	n.i.	10	64	n.i.	
		R	23	11	88	n.i.			R	18	n.i.	10	17	

Table 1. continued

	Substituent	NS2B-NS3	Thr	<i>E. coli</i> MurA	<i>E. coli</i> MetAP		Substituent	NS2B-NS3	Thr	<i>E. coli</i> MurA	<i>E. coli</i> MetAP		
35		T	25	14	11	66	36		T	18	16	17	27
		R	35	18	14	21							
37		T	30	18	16	20	38		T	12	n.i.	13	58
		R	22	29	13	40							
		Td	25	n.i.	n.i.	n.i.							
39		R	n.i.	11	n.i.	n.i.	40		T	44	23	15	n.i.
		T	n.i.	23	29	18							
41		R	n.i.	20	69	n.i.	42		T	n.i.	n.i.	n.i.	24
		T	n.i.	23	29	18							
43		T	37	38	69	23	44		T	13	18	48	27
		R	26	28	94	14							
		Td	n.i.	24	24	12							

^aShown are the respective substituents at the α -carbon of the heterocycles (cf. Figure 1). The activities are color-coded to facilitate a quick overview. E, enzyme; I, inhibitor; Thr, thrombin; n.i., no inhibition; n.d., not determined. Concentrations for NS2B-NS3: E, 100 nM; I, 50 μ M. Concentrations for Thr: E, 10 nM; I, 25 μ M. Concentrations for *E. coli* MurA: E, 12 nM; I, 25 μ M. Concentrations for *E. coli* MetAP: E, 500 nM; I, 10 μ M. Legend for the color code is as follows:



SAR of Aromatic FMMHs: Table 1. Considering the two serine proteases (NS2B-NS3 and thrombin) in the panel, the SAR of the aromatic FMMHs appears quite "flat". The substituent at the α -carbon has only a minor influence on the activity, and highly diverse substituents result in similar inhibitory potencies. The inhibitory activity against NS2B-NS3 is generally somewhat more pronounced than against thrombin, which may also be due to the higher concentration of the tested compounds in the NS2B-NS3 assay. Thiohydantoin and rhodanine derivatives are usually more potent against thrombin and NS2B-NS3 than hydantoins and thiazolidinediones.

For the other two enzymes, the SAR landscape appears considerably more rugged, with the α -substituent having a pronounced influence on the activity. In the case of the bacterial transferase *E. coli* MurA, considerable activities and selectivities can be observed for derivatives of all types of heterocycles. There is a strong sensitivity to minor changes at the α -substituent, as can be seen for the closely related thiazolidinediones **13Td**–**19Td**. A clear preference of MurA for one of the FMMH heterocycles is not evident.

The metalloprotease MetAP shows a very pronounced selectivity for a few compounds that contain highly specific structural features. These are polyphenolic functionalities as in all compounds bearing the dihydroxyphenyl moiety (**18T/R/H/Td**), irrespective of the FMMH but also the pyridine and imidazole congeners **29T** and **31T**. These structural features are highly prone to form interactions with the native or auxiliary metal ions in the MetAP active site.²⁹

SAR of Nonaromatic FMMHs: Table 2. All compounds with nonaromatic heterocycle are practically inactive against the

two serine proteases. The two dihydroxyphenyl derivatives **56** and **57** inhibit *E. coli* MurA and MetAP. This can be seen as analogy to compounds **18T/R/H/Td** which have a similar spectrum of activity. In the case of MetAP, the activity can again be explained by a binding of the phenolic hydroxy groups to the metal ions in the active site.

Conclusions Derived from the Enzyme Inhibition Data.

The SAR landscapes of the FMMH derivatives cannot generally be described as "flat", since the activity at MurA and MetAP strongly depends on the α -substituent. The FMMH is apparently not critical for the interaction with these two targets. In contrast, thrombin and NS2B-NS3 strongly (and nearly solely) depend on the presence of an FMMH scaffold, and the aromaticity of the heterocycle appears to be an essential feature.

No Unspecific Reactivity toward Biological Nucleophiles. The exocyclic double bond in the compounds of Table 1 is in conjugation with a keto group, and it may thus be argued that it is prone to react with biological nucleophiles (Michael addition). A covalent bond between an unsaturated rhodanine and a cysteine residue of HCV polymerase has been described by Powers and co-workers (cf. PDB code 2AWZ).³⁰ To study this possibility, the reactivity toward glutathione as an exemplary biological nucleophile was determined for a selection of 14 compounds with high activity against one or more enzymes. There was no reaction detectable; we therefore judge the electrophilicity of this Michael system to be insignificant. A reaction in this position would destroy the aromatic system of the ring and is therefore very unfavorable.

No Aggregation-Based Promiscuity. A frequently encountered mode of promiscuous inhibition depends on the

Table 2. Inhibition of Four Enzymatic Targets by 23 FMMH Derivatives with Nonaromatic Heterocycles^a

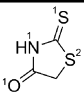
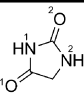
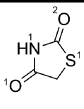
	Structure	NS2B-NS3	Thr	<i>E. coli</i> MurA	<i>E. coli</i> MetAP		Structure	NS2B-NS3	Thr	<i>E. coli</i> MurA	<i>E. coli</i> MetAP
T		n.i.	n.i.	n.i.	n.i.	R		14	n.i.	n.i.	n.i.
H		n.i.	n.i.	n.i.	n.i.	Td		13	n.i.	n.i.	n.i.
45		n.i.	n.i.	n.i.	13	45a		n.i.	n.i.	20	n.i.
46		n.i.	n.i.	n.i.	13	46a		10	n.i.	25	n.i.
47		n.i.	n.i.	19	12	47a		n.i.	n.i.	17	12
48		n.i.	n.i.	15	n.i.	48a		14	12	11	n.i.
52		n.i.	n.i.	n.i.	22	53		n.i.	n.i.	n.i.	n.i.
54		n.i.	n.i.	n.i.	n.i.	55		n.i.	n.i.	11	n.i.
49		n.i.	n.i.	12	n.i.	49a		11	n.i.	n.i.	n.i.
51		n.i.	n.i.	n.i.	n.i.	51a		n.i.	n.i.	n.i.	n.i.
56		15	n.i.	63	73	57		n.i.	n.i.	79	84
58		n.i.	n.i.	n.i.	n.i.	59		n.i.	n.i.	n.i.	n.i.
50		n.i.	n.i.	n.i.	n.i.	50a		n.i.	n.i.	11	13
60		n.i.	n.i.	n.i.	19						

^aE, enzyme; I, inhibitor; Thr, thrombin; n.i., no inhibition; n.d., not determined. Concentrations for NS2B-NS3: E, 100 nM; I, 50 μ M. Concentrations for Thr: E, 10 nM; I, 25 μ M. Concentrations for *E. coli* MurA: E, 12 nM; I, 25 μ M. Concentrations for *E. coli* MetAP: E, 500 nM; I, 10 μ M. Legend for the color code is as follows:

36-39% 40-49% 50-59% 60-69% 70-79% 80-89% 90-99% 100%



Table 3. Interactions of the Heavy Atoms of FMMHs in Protein–Ligand Crystal Structures

Structure of FMMH and number of protein–ligand X-ray structures												
	O1	N1	S1	S2	O1	N1	O2	N2	O1	N1	O2	S1
Number of interactions made by the specified atom in all protein–ligand complexes	8	4	21	1	23	14	24	0	21	8	13	0
Average number of interactions made by the specified atom	0.89	0.44	2.33	0.11	1.64	1.00	1.71	0.00	1.91	0.73	1.18	0.00

formation of multimolecular aggregates. The aggregates attach to the target surfaces, which leads to inactivation in a highly unspecific way.⁶ To determine whether this may be a factor in the present case, we investigated 35 compounds that interfered with all four targets by dynamic light scattering. Dynamic light scattering (DLS) is an analytical method to determine particle size in solution, so the aggregation behavior of a compound can be observed. We found **1H** and **12Td** (and the reference compounds quercetin and curcumin) to be the only ones showing a limited degree of aggregation. This observation can explain the “selective” inactivation of the *E. coli* MurA by compound **1H** because the MurA assay is the only detergent-free assay in this panel, and detergents can be used to minimize aggregation-based promiscuous inhibition.^{31,32} However, aggregation-based promiscuity cannot be a relevant factor for the other compounds in this data set, since DLS was negative.

Binding Modes of FMMH Derivatives in Protein–Ligand Complexes. Two features appear to be essential for the multitarget-binding profile of FMMH derivatives. First, the heterocycle is aromatic. Second, the heterocycle should contain an exocyclic, double-bonded sulfur atom as in the rhodanines and thiohydantoin. To understand these requirements, we analyzed the published X-ray protein–ligand cocrystal structures of FMMH derivatives from the PDB. A complete list is given in the Supporting Information, and a summary is provided in Table 3. We were unable to find cocrystal structures that contained ligands carrying the thiohydantoin scaffold. The other FMMH scaffolds were found in 34 cocrystal structures, with 9 rhodanines, 14 hydantoin, and 11 thiazolidinediones. It is highly remarkable that all hydantoin derivatives are saturated (no C–C double bond at the α -carbon) whereas all rhodanines and most thiazolidinediones are unsaturated. It therefore, again, seems that the combination of exocyclic sulfur with an aromatic heterocycle is associated with a very particular binding behavior.

We determined the number of interactions toward the target protein of every heavy atom in the FMMH scaffold and in the other substituents of the molecules (Tables 3 and 4). The interactions to the FMMH scaffolds were mostly polar (electrostatic or hydrogen bond; see Supporting Information for details). A most interesting comparison can be made between rhodanines and thiazolidinediones, which differ only in the exchange of the exocyclic sulfur against oxygen (S1 vs O2). This exchange leads to a dramatic loss of interactions, with S1 in the rhodanines making an average of 2.33 interactions, but O2 in the thiazolidinediones making only an average of 1.18 interactions. We can therefore conclude that the exocyclic, double-bonded S1 in the rhodanines, and most likely also the corresponding sulfur in the thiohydantoin, has a pronounced propensity to form polar, intermolecular interactions.

Table 4. Interaction Statistics of the FMMH Scaffold and the Remainder of FMMH Derivatives in the Brookhaven Database (PDB)

	FMMH	Remainder of Ligand
Total number of interactions made by the fragment in 33 ligands	137	127
Average number of interactions made by the fragment	4.28	4.10
Average number of heavy atoms in the respective fragment	7.00	17.8
Average number of interactions per heavy atom in the fragment	0.61	0.23

Another type of analysis (cf. Table 4) deals with the relative contributions of the FMMH scaffold and the remainder of the cocrystal ligands to the binding effect. We counted the number of interactions of the FMMH scaffold and the remainder of the ligand and set these numbers in relation to the number of heavy atoms (C, N, O, S) in these fragments (Table 4). The FMMH scaffolds make an average number of 4.28 interactions, or 0.61 interactions per heavy atom. In contrast, the density of interactions is much lower for the remainder of the ligand, which makes an average of 4.1 interactions. The remainder of the ligand is usually much larger than the FMMH (7 vs 17.8 heavy atoms), and thus, the average number of interactions per heavy atom is considerably lower for the remainder (0.23 per heavy atom). This analysis is far from perfect because a simple “counting” of interactions is not capable of measuring the particular energetics that are associated with every interaction and because hydrophobic interactions are underestimated. Nevertheless, this analysis demonstrates that the FMMHs confer a very significant amount of spatially defined intermolecular interactions and that the density of such interactions is very high in comparison to the other fragments of the ligands.

DFT Study of FMMH Derivatives. To further understand the exceptional properties of FMMHs with exocyclic sulfur atoms, we performed DFT calculations on benzyldene- and benzyl-substituted analogues. A variety of electronic properties, including HOMO and LUMO localization, electron localization function (ELF), electrostatic potential, and total electron density were analyzed. The most revealing analysis, which also reflects the other electronic properties, is the electrostatic potential mapped on the surface-accessible molecular surface and the localization of the HOMO orbitals (cf. Figure 3). The HOMO orbital and the negative electrostatic potential are strongly localized at the exocyclic sulfur in the rhodanines and thiohydantoin. The spatial distribution of these electronic properties is much more diffuse in the other two FMMH derivatives. We therefore conclude that at least a part of the exceptional biomolecular binding properties of the rhodanines and thiohydantoin is due to the special

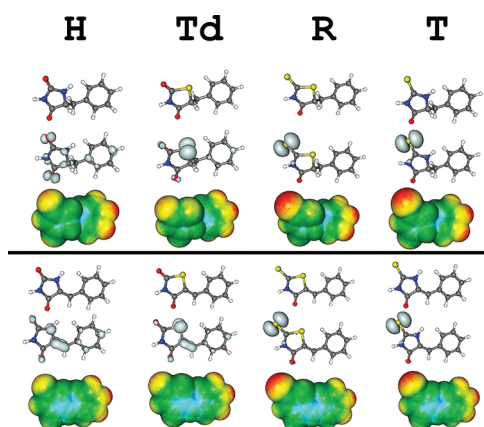


Figure 3. Optimized structures, localization of HOMO orbitals, and the electrostatic potential mapped on the van der Waals surface of representative FMMHs: (top row) benzyl substituent at $C\alpha$; (bottom row) benzylidene substituent at $C\alpha$. Calculations were performed using CPMD³³ and visualization was by Molekel.³⁴

electronic properties that are conferred by the exocyclic, double-bonded sulfur.

Hydrogen Bonding of C=S versus C=O. The scientific literature contains a number of publications that deal with the comparison of double-bonded oxygen versus sulfur atoms as hydrogen-bond acceptors. These publications are based on the analysis of small-molecular X-ray structures and theoretical calculations on small molecules, but we were unable to identify previous studies that deal with the analysis of C=S vs C=O in protein–ligand interactions. For example, Allen et al.^{35,36} and Custalcean³⁷ find significant differences in the H-bond acceptor properties of C=S and C=O, with the sulfur having a more diffuse lone pair electron density distribution around the sulfur and frequently interacting with three and four hydrogen-bond-donor groups. These authors calculate the energetics of a hydrogen bond to sulfur in C=S to be inferior to those of oxygen in C=O. However, in the context of protein–ligand-interactions, the desolvation of the ligand has to be considered (breaking of hydrogen bonds to water prior to protein binding), and the free energy penalty of breaking a “strong” C=O hydrogen bond to water may result in the overall ligand binding process being more favorable for the C=S group. In water, the stricter geometric requirements of the C=O group as hydrogen bond acceptor can more easily be satisfied than in protein–ligand complexes. When a ligand has to “adjust” to a geometry that is predefined by a proteinaceous receptor, the more geometrically tolerant C=S group, which is also able to form a larger number of hydrogen-bonds, has more flexibility to adjust its intermolecular interactions to the given requirements.

CONCLUSIONS

We conclude that the five-membered multiheterocycles that contain an exocyclic sulfur atom, such as the rhodanines and thiohydantoin, possess a distinct intermolecular interaction profile. This is particularly pronounced if the heterocycle becomes aromatic, such as in the benzylidene rhodanines. The distinct binding profile is clearly not related to “unspecific” properties such as aggregation or reactivity, but rather (as could be shown by a detailed analysis of protein–ligand structures and the literature data on small molecules) to electronic and hydrogen-bonding properties that can be explained and understood. We therefore think that rhodanines and related

scaffolds should not be regarded as problematic or promiscuous binders per se. However, it is important to note that the intermolecular interaction profile of these scaffolds makes them prone to bind to a large number of targets with weak or moderate affinity. It may be that the observed moderate affinities of rhodanines and related compounds, e.g., in screening campaigns, have been overinterpreted in the past and that these compounds have too easily been put forward as lead compounds for further development. We suggest that particularly strong requirements, i.e., affinity in the lower nanomolar range and proven selectivity for the target, are applied in the further assessment of rhodanines and related compounds. A generalized “condemnation” of these chemotypes, however, appears inadequate and would deprive medicinal chemists from attractive building blocks that possess a remarkably high density of intermolecular interaction points.

EXPERIMENTAL SECTION

General. All enzymes except thrombin were expressed and purified in our laboratory as described previously.^{4,5,28} Thrombin (from bovine plasma) was purchased from Sigma-Aldrich. Experiments were performed in triplicate ($n = 3$), and the experimental values were averaged. Standard deviations were generally $\leq 10\%$.

Dengue Virus (DenV) Protease Assay. The DenV protease assay was performed as described previously (Steuer et al.) in the presence of detergent (0.0016% Brij 58). In short, continuous enzymatic assays were performed on a BMG Labtech Fluostar OPTIMA microtiter fluorescence plate reader using black 96-well V-bottom plates from Greiner. The protease was assayed using the substrate Abz-NleKRRS-3-(NO₂)Y, which we synthesized according to routine solid phase peptide synthesis protocols. The excitation wavelength was 320 nm, and the emission was monitored at 405 nm. The inhibitor concentration was 50 μM . The inhibitors were preincubated for 15 min with the enzyme. Afterward, the reaction was initiated by the addition of the substrate to a final concentration of 50 μM . The activity of the enzyme was determined as the initial slope per second and monitored for 15 min.

Thrombin Assay. The thrombin assay was performed as a continuous fluorimetric assay on a BMG Labtech Fluostar OPTIMA microtiter fluorescence plate reader. The excitation wavelength was 355 nm, and the emission wavelength was 460 nm. The protease was assayed using the substrate Boc-Val-Pro-Arg-AMC (Bachem, Germany). The final concentrations of the enzyme and substrate were 10 nM and 50 μM , respectively. The inhibitors were preincubated with the enzyme for 15 min at 25 μM . The cleavage reaction was initiated by addition of the substrate. The assay buffer consisted of 50 mM Tris-HCl, pH 7.5, 150 mM NaCl, and a detergent (0.05% Tween 20) as described by Diamond.³⁸ The activity of the enzyme was determined as the initial slope per second and monitored for 10 min.

MurA Assay. *E. coli* UDP-N-acetylglucosaminocarboxyvinyl transferase (MurA) (15 nM) was preincubated with 31.25 mM Tris, pH 7.8, 312.5 μM UNAG, 0.125% BSA, and inhibitor (10 μL , aqueous solution containing 10% DMSO) or without inhibitor (10 μL , water with 10% DMSO) for 10 min at 37 °C. The reaction was started by the addition of the second substrate PEP (20 μL , 625 μM), resulting in a total volume of 100 μL with the following concentrations: *E. coli* MurA 12 nM, BSA 0.1%, UNAG 250 μM , PEP 125 μM , Tris 25 mM, pH 7.8, DMSO 1%. This assay buffer did not contain a detergent. The reaction was stopped after 60 min at 37 °C by adding 100 μL of Lanzetta reagent. The absorbance at 620 nm was measured using a BMG Labtech Fluostar multiplate reader to quantify the released inorganic phosphate. KH₂PO₄ was utilized as a standard.

Methionine Aminopeptidase (MetAP) Assay. An amount of 10 μL of MetAP (5 μM) was preincubated with 10 μL of inhibitor (100 μM containing 1% DMSO) and 60 μL of a mixture containing 50 mM Tris maleate, pH 7.5, 0.16 M NaCl, 0.16 mM CoCl₂, and 0.125% BSA for 30 min at 37 °C. The reaction was started by the addition of 20 μL of Met-AMC (1 mM containing 5% DMSO),

resulting in a total volume of 100 μL with the following concentrations: *E. coli* MetAP 500 nM, Tris maleate 50 mM, pH 7.5, 0.1 M NaCl, 0.1 mM CoCl_2 , 0.075% BSA, 0.2 mM Met-AMC, 10 μM inhibitor, and 1.1% DMSO. This assay buffer did not contain a detergent. The continuous assay was performed for 15 min at 37 °C on a BMG Labtech Fluostar OPTIMA microtiter fluorescence plate reader using black 96-well V-bottom plates from Greiner. The excitation wavelength was 360 nm, and the emission was monitored at 460 nm. The activity of the enzyme was determined as initial slope per second.

Dynamic Light Scattering (DLS) Measurements. Inhibitors were diluted from 10 mM stocks in DMSO with filtered 50 mM KPi buffer, pH 7, to a final concentration of 50 μM . All measurements were performed at room temperature using a Zetasizer 3000 HS (Malvern Instruments GmbH, Herrenberg, Germany). The laser power and integration times were comparable for all experiments. The scattering angle was 173°. The analyzed compounds were 1T, 1R, 1H, 1Td, 8T, 10T, 10R, 10H, 10Td, 12T, 12R, 12H, 12Td, 17R, 18T, 18R, 18H, 19T, 19R, 19H, 19Td, 21R, 21T, 22R, 23T, 23R, 25T, 25R, 25Td, 29T, 31T, 31R, 33T, 33R, 43R.

Glutathione Binding Study. The compounds were incubated with glutathione in DenV assay buffer, and samples were removed after 0, 30, 120, and 240 min. The reaction was stopped by addition of 4% trifluoroacetic acid to a final concentration of 0.1% and analyzed by RP-HPLC with detection by UV at 254 nm. The reaction progress was followed by decrease of the educt signal with the 0 min value as reference. The analyzed compounds were 1H, 10T, 10R, 10H, 10Td, 12R, 13T, 13R, 13H, 13Td, 14T, 14R, 14H, 14Td.

Theoretical Methods. The RCSB protein database (PDB)³⁹ was scanned using SMILES representations for crystallographic ligands that contain FMMH substructures. The hits were downloaded, and hydrogens were added using the HBPredICT, version 1.1, software.⁴⁰ Compounds in which the FMMH was part of a spiro ring system were excluded. Interactions between the compounds and the macromolecular structures were visualized and analyzed using PyMol.⁴¹

The DFT-based Car–Parrinello⁴² molecular dynamics program CPMD, version 3.11, was used for the DFT calculations.³³ CPMD parameters were the following: isolated system calculations; gradient-corrected exchange-correlation functionals due to Becke and Lee, Yang, and Parr (BLYP);^{43,44} plane waves basis set; fictitious electron mass 400 au; the convergence criterion for geometry optimization (GDIIS/BFGS algorithm) was a gradient below 5×10^{-4} au; the size of the cubic QM box was $16 \text{ \AA} \times 16 \text{ \AA} \times 16 \text{ \AA}$, corresponding to a minimum image distance of about 9 \AA . Visualization was done with Molekel.³⁴

Chemistry. The NMR spectra were recorded at room temperature on a Varian Mercury Plus (300 MHz) or Varian NMR system 500 (500 MHz) spectrometer with CDCl_3 , CD_3OD , D_2O , acetone- d_6 , or DMSO- d_6 as internal standard. Chemical shifts (δ) are given in ppm. Coupling constants are in hertz, and splitting patterns are designated as follows: s, singlet; bs, broad singlet; d, doublet; dd, doublet of doublets; t, triplet; dt, doublet of triplets q, quartet; m, multiplet. Data were interpreted with MestReC, version 4.9.9.9. Microwave-assisted syntheses were performed in an Anton Paar Monowave 300 reactor. The reaction progress was determined by thin layer chromatography on Merck silica gel plastic plates 60 F₂₅₄ (detection by UV and KMnO_4). Column chromatography was performed on silica (0.060–0.200 mm, 60 \AA) with a Biotage Isolera One purification system. HPLC was performed on an Agilent 1200 HPLC system with a MWD (Agilent, Santa Clara, CA, U.S.). As stationary phase a XTerra RP-18 column (100 mm \times 3 mm, 2.5 μm) was used, and a linear gradient from 10% to 98% B over 10 min with a flow rate of 0.8 mL/min and A consisting of water (0.1% formic acid) and B consisting of acetonitrile (0.1% formic acid) as solvents was performed. The purity of the compounds was determined by HPLC (detection by UV at 254 nm) and $\geq 95\%$ unless otherwise indicated. EI mass spectra were recorded by Heiko Rudy on a Finnigan MAT 8200 instrument. High resolution mass spectra were recorded on a Bruker micrOTOF II instrument with sodium formate as calibrant. Small molecule X-ray structures were recorded and analyzed by Dr. Frank Rominger at the Department of

Chemistry, University of Heidelberg, Germany, on a Siemens CCD diffractometer.

Procedure A: Synthesis of 1-Acetyl-2-thiohydantoin. Thiohydantoin were synthesized out of several amino acids (2.53 mmol), sodium thiocyanate (5.07 mmol), and acetic anhydride as solvent. This mixture was stirred under reflux for 1 h. After cooling to room temperature, the solution was added to 40 mL of an ice/water mix and stored overnight in a freezer. The resulting precipitate was filtered and dried under vacuum. If necessary, the product was purified by column chromatography.

Procedure B: Deacetylation of 1-Acetyl-2-thiohydantoin. For deacetylation, the synthesized 1-acetyl-2-thiohydantoin were dissolved in hydrochloric acid (3 M) and stirred under reflux for 1 h, followed by a common workup procedure.

Procedure C: Synthesis of Substituted Thiohydantoin. A mixture of 1-acetyl-2-thiohydantoin (0.95 mmol), NH_4OAc (1.89 mmol), and the appropriate aldehyde or ketone (1.05 mmol) in 15 mL of concentrated acetic acid was heated to 160 °C for 5 min under microwave irradiation. The resulting precipitate was washed with water and dried under vacuum. If necessary, the product was purified by flash chromatography.

Procedure D: Synthesis of Substituted Rhodanines. A mixture of rhodanine (1.13 mmol), NH_4OAc (2.25 mmol), and the appropriate aldehyde or ketone (1.24 mmol) in 15 mL of toluene was heated to 160 °C for 5 min under microwave irradiation. The resulting precipitate was washed with water and dried under vacuum. If necessary, the product was purified by flash chromatography.

Procedure E: Synthesis of Substituted Hydantoin. A mixture of hydantoin (1.50 mmol), NH_4OAc (3.00 mmol), and the appropriate aldehyde or ketone (1.65 mmol) in 15 mL of toluene was heated 3 times to 200 °C for 20 min under microwave irradiation. The resulting precipitate was washed with water and dried under vacuum. If necessary, the product was purified by flash chromatography.

Procedure F: Synthesis of Substituted Thiazolidinediones. A mixture of 2,4-thiazolidinedione (1.28 mmol), NH_4OAc (2.56 mmol), and the appropriate aldehyde or ketone (1.41 mmol) in 15 mL of toluene was heated to 170 °C for 5 min under microwave irradiation. The resulting precipitate was washed with water and dried under vacuum. If necessary, the product was purified by flash chromatography.

Preparation of Exemplary Compounds. 5-Benzylidene-2-thioxoimidazolidin-4-one (1T). 1T was synthesized according to procedure C in 61% yield. ¹H NMR (300 MHz, DMSO- d_6): δ = 6.49 (s, 1H), 7.40 (m, 3H), 7.75 (dd, J = 8.0 Hz, J = 1.4 Hz, 2H), 12.25 (bs, 2H). ¹³C NMR (75 MHz, DMSO- d_6): δ = 111.4, 127.7, 128.7, 129.1, 130.1, 132.2, 165.7, 179.2. HRMS (ESI, $[\text{M} - \text{H}]^-$) calcd ($\text{C}_{10}\text{H}_8\text{N}_2\text{OS}$) 203.0285; found 203.0291.

5-Benzylidene-2-thioxothiazolidin-4-one (1R). 1R was synthesized according to procedure D in 68% yield. ¹H NMR (300 MHz, DMSO- d_6): δ = 7.54 (m, 6H). ¹³C NMR (125 MHz, DMSO- d_6): δ = 125.4, 129.3, 130.4, 130.6, 131.5, 132.9, 169.3, 195.6. HRMS (ESI, $[\text{M} - \text{H}]^-$) calcd ($\text{C}_{10}\text{H}_7\text{NOS}_2$) 219.9896; found 219.9894.

5-Benzylidenethiazolidine-2,4-dione (1Td). 1Td was synthesized according to procedure F in 88% yield. ¹H NMR (300 MHz, DMSO- d_6): δ = 7.54 (m, 5H), 7.79 (s, 1H), 11.9 (s, 1H). ¹³C NMR (125 MHz, DMSO- d_6): δ = 123.5, 129.2, 129.9, 130.3, 131.7, 132.9, 167.2, 167.8. HRMS (ESI, $[\text{M} - \text{H}]^-$) calcd ($\text{C}_{10}\text{H}_7\text{NO}_2\text{S}$) 204.0125; found 204.0128.

5-(1-Phenylethylidene)-2-thioxoimidazolidin-4-one (2T). 2T was synthesized according to procedure C in 2% yield. ¹H NMR (300 MHz, acetone- d_6): δ = 2.53 (s, 3H), 7.44 (m, 5H). ¹³C NMR (75 MHz, acetone- d_6): δ = 18.9, 129.5, 129.6, 129.9, 130.2, 130.8, 131.1, 134.8, 141.2. HRMS (ESI, $[\text{M} - \text{H}]^-$) calcd ($\text{C}_{11}\text{H}_{10}\text{N}_2\text{OS}$) 217.0441; found 217.0444.

5-(3,4-Dihydroxybenzylidene)-2-thioxoimidazolidin-4-one (18T). 18T was synthesized according to procedure C in 92% yield. ¹H NMR (300 MHz, CD_3OD): δ = 6.46 (s, 1H), 6.84 (d, J = 8.0 Hz, 1H), 7.01 (s, 1H), 7.04 (d, J = 8.1 Hz, 1H). ¹³C NMR (75 MHz, DMSO- d_6): δ = 113.3, 115.8, 117.7, 122.8, 123.7, 125.3, 145.4, 147.5, 165.7, 178.1. HRMS (ESI, $[\text{M} - \text{H}]^-$) calcd ($\text{C}_{10}\text{H}_8\text{N}_2\text{O}_3\text{S}$) 235.0183; found 235.0181.

5-(3,4-Dihydroxybenzylidene)-2-thioxothiazolidin-4-one (18R). 18R was synthesized according to procedure D in 88% yield. ¹H NMR (300 MHz, CD₃OD): δ = 6.86 (d, *J* = 8.2 Hz, 1H), 6.94 (dd, *J* = 8.2 Hz, *J* = 1.8 Hz, 1H), 6.99 (d, *J* = 2.1 Hz, 1H), 7.41 (s, 1H). ¹³C NMR (75 MHz, DMSO-*d*₆): δ = 116.4, 116.5, 120.7, 124.3, 124.9, 132.7, 145.9, 149.1, 169.5, 195.5. HRMS (ESI, [M - H]⁻) calcd (C₁₀H₇N₂O₃S₂) 251.9795; found 251.9797.

5-(3,4-Dihydroxybenzylidene)imidazolidine-2,4-dione (18H). 18H was synthesized according to procedure E in 35% yield. ¹H NMR (300 MHz, acetone-*d*₆): δ = 6.40 (s, 1H), 6.86 (d, *J* = 8.2 Hz, 1H), 7.01 (dd, *J* = 8.2 Hz, *J* = 2.1 Hz, 1H), 7.07 (d, *J* = 2.1 Hz, 1H). ¹³C NMR (75 MHz, DMSO-*d*₆): δ = 109.8, 115.8, 117.2, 121.4, 124.3, 125.5, 145.3, 146.4, 155.9, 165.6. HRMS (ESI, [M - H]⁻) calcd (C₁₀H₈N₂O₄) 219.0411; found 219.0413.

5-(3,4-Dihydroxybenzylidene)thiazolidine-2,4-dione (18Td). 18Td was synthesized according to procedure F in 67% yield. ¹H NMR (300 MHz, CD₃OD): δ = 6.86 (d, *J* = 8.2 Hz, 1H), 6.95 (dd, *J* = 8.3 Hz, *J* = 2.0 Hz, 1H), 7.01 (d, *J* = 2.0 Hz, 1H), 7.41 (s, 1H). ¹³C NMR (75 MHz, CD₃OD): δ = 117.2, 117.7, 120.6, 125.4, 126.5, 134.3, 147.2, 149.8, 169.2, 169.8. HRMS (ESI, [M - H]⁻) calcd (C₁₀H₇N₂O₄S) 236.0023; found 236.0024.

5-(3-Chlorothiophen-2-yl)methylene)-2-thioxoimidazolidin-4-one (24T). 24T was synthesized according to procedure C in 45% yield. ¹H NMR (300 MHz, CD₃OD): δ = 6.78 (s, 1H), 7.13 (d, *J* = 5.4 Hz, 1H), 7.75 (d, *J* = 5.4 Hz, 1H). ¹³C NMR (75 MHz, CD₃OD): δ = 101.9, 128.9, 129.5, 129.6, 130.4, 130.7, 167.2, 180.5. HRMS (ESI, [M - H]⁻) calcd (C₈H₅ClN₂O₂S₂) 242.9459; found 242.9457.

5-((3-Chlorothiophen-2-yl)methylene)-2-thioxothiazolidin-4-one (24R). 24R was synthesized according to procedure D in 31% yield. ¹H NMR (300 MHz, DMSO-*d*₆): δ = 7.39 (d, *J* = 5.3 Hz, 1H), 7.63 (s, 1H), 8.20 (d, *J* = 5.2 Hz, 1H). ¹³C NMR (75 MHz, DMSO-*d*₆): δ = 119.9, 125.9, 129.8, 130.6, 130.8, 134.2, 169.4, 194.5. HRMS (ESI, [M - H]⁻) calcd (C₈H₄ClNOS₃) 259.9071; found 259.9071.

5-((3-Chlorothiophen-2-yl)methylene)imidazolidine-2,4-dione (24H). 24H was synthesized according to procedure E in 25% yield. ¹H NMR (300 MHz, CD₃OD): δ = 6.81 (s, 1H), 7.09 (d, *J* = 5.4 Hz, 1H), 7.67 (d, *J* = 5.4 Hz, 1H). ¹³C NMR (75 MHz, CD₃OD): δ = 112.0, 127.9, 129.0, 129.1, 129.4, 130.7, 166.6, 173.4. HRMS (ESI, [M - H]⁻) calcd (C₈H₅ClN₂O₂S) 226.9687; found 226.9690.

5-((3-Chlorothiophen-2-yl)methylene)thiazolidine-2,4-dione (24Td). 24Td was synthesized according to procedure F in 26% yield. ¹H NMR (300 MHz, CD₃OD): δ = 7.19 (d, *J* = 5.4 Hz, 1H), 7.88 (d, *J* = 5.4 Hz, 1H), 6.98 (s, 1H). ¹³C NMR (75 MHz, DMSO-*d*₆): δ = 120.9, 124.0, 129.4, 130.3, 130.8, 132.6, 167.2, 167.5. HRMS (ESI, [M - H]⁻) calcd (C₈H₄ClNO₂S₂) 243.9282; found 243.9280.

(S)-1-Acetyl-5-benzyl-2-thioxoimidazolidin-4-one (47). 47 was synthesized according to procedure A. Yield 93%. ¹H NMR (300 MHz, DMSO-*d*₆): δ = 2.69 (s, 3H), 3.12 (m, 1H), 3.40 (m, 1H), 4.99 (m, 1H), 6.97 (m, 2H), 7.77 (m, 3H), 12.42 (s, 1H). ¹³C NMR (75 MHz, DMSO-*d*₆): δ = 27.8, 34.9, 63.9, 127.7, 128.8, 129.7, 134.6, 170.5, 172.9, 182.7. MS (EI): *m/z* = 248.10 g/mol [M⁺].

(S)-5-Benzyl-2-thioxoimidazolidin-4-one (47a). 47a was synthesized according to procedure B out of 47. Yield 87%. ¹H NMR (300 MHz, DMSO-*d*₆): δ = 2.95 (d, 2H, *J* = 5.0 Hz), 4.54 (m, 1H), 7.20 (m, 5H), 10.04 (s, 1H), 11.41 (s, 1H). ¹³C NMR (75 MHz, DMSO-*d*₆): δ = 35.6, 61.3, 126.7, 128.0, 129.5, 134.9, 175.6, 182.1. MS (EI): *m/z* = 206.10 g/mol [M⁺].

(S)-5-(4-Hydroxybenzyl)-2-thioxoimidazolidin-4-one (51a). 51a was synthesized according to procedures A and B. Yield 88%. ¹H NMR (300 MHz, acetone-*d*₆): δ = 2.98 (d, *J* = 4.0 Hz, 2H), 4.07 (t, *J* = 4.0 Hz, 1H), 6.71 (d, *J* = 4.0 Hz, 2H), 7.04 (d, *J* = 4.0 Hz, 2H). HRMS (ESI, [M - H]⁻) calcd (C₁₀H₁₀N₂O₂S) 221.0363; found 221.0363.

(S)-5-Benzylimidazolidine-2,4-dione (52). See procedure for 53. Yield 61%. ¹H NMR (300 MHz, DMSO-*d*₆): δ = 2.92 (dd, 2H, *J* = 4.8 Hz, *J* = 2.2 Hz), 4.32 (t, 1H, *J* = 5.1 Hz), 7.22 (m, 5H), 7.91 (bs, 1H), 10.4 (bs, 1H). ¹³C NMR (75 MHz, DMSO-*d*₆): δ = 36.2, 58.3, 126.5, 127.9, 129.6, 135.5, 157.0, 175.1. HRMS (ESI, [M - H]⁻) calcd (C₁₀H₉N₂O₂) 189.0742; found 189.0668.

(R)-5-Benzylimidazolidine-2,4-dione (53). A mixture of L-phenylalanine (3.03 mmol) and sodium cyanate (6.06 mmol) in water (20 mL) was heated to 50 °C and stirred for 30 min. The solution was evaporated to 5 mL, and 1 M HCl was added dropwise until a precipitate remained. Afterward 2 M HCl (10 mL) was added and the suspension was refluxed for 2 h. The reaction mixture was allowed to cool to room temperature and the resulting precipitate was collected, washed with water, and dried under vacuum to obtain 53. Yield 72%. ¹H NMR (300 MHz, DMSO-*d*₆): δ = 2.92 (dd, 2H, *J* = 4.8 Hz, *J* = 2.2 Hz), 4.32 (t, 1H, *J* = 5.1 Hz), 7.22 (m, 5H), 7.91 (bs, 1H), 10.4 (bs, 1H). ¹³C NMR (75 MHz, DMSO-*d*₆): δ = 36.2, 58.3, 126.5, 127.9, 129.6, 135.5, 157.0, 175.1. HRMS (ESI, [M - H]⁻) calcd (C₁₀H₉N₂O₂) 189.0742; found 189.0667.

5-Benzylthiazolidine-2,4-dione (54). To a solution of 2,4-thiazolidinedione (4.20 mmol) at -78 °C was added *n*-butyllithium (8.40 mmol) dropwise and stirred for 15 min. The reaction mixture was then placed in an ice bath for 30 min. When the mixture was cooled to -78 °C, benzyl bromide (4.20 mmol) was added and the mixture was stirred for 30 min. The reaction mixture was allowed to warm to room temperature and stirred for additional 90 min. The reaction was quenched with 5% sulfuric acid and the aqueous phase extracted with ethyl acetate. The organic layer was dried and concentrated. Column chromatography furnished 54. Yield 52%. ¹H NMR (300 MHz, DMSO-*d*₆): δ = 3.12 (dd, 1H, *J* = 14.1 Hz, *J* = 9.2 Hz), 3.39 (dd, 1H, *J* = 14.1 Hz, *J* = 4.4 Hz), 4.92 (dd, 1H, *J* = 9.3 Hz, *J* = 4.4 Hz), 7.29 (m, 5H), 10.4 (bs, 1H). ¹³C NMR (75 MHz, DMSO-*d*₆): δ = 37.0, 52.6, 126.9, 128.3, 129.1, 136.8, 171.5, 175.6. HRMS (ESI, [M - H]⁻) calcd (C₁₀H₉N₂O₂S) 206.0354; found 206.0277.

5-Benzyl-2-thioxothiazolidin-4-one (55). An amount of 1.87 mL ammonia (7 M in MeOH) was added to 10 mL of EtOH and cooled to 0 °C. To this solution was added dropwise a precooled mixture of carbon disulfide (26.2 mmol) in 5 mL of ether. The reaction mixture was stirred for 2 h at 0 °C and overnight at room temperature. The resulting precipitate was collected, sucked dry, and transferred to a solution of 2-bromo-3-phenylpropanoic acid (2.24 mmol) in water and stirred for 2 h. The solution was transferred to 6 M HCl (80 °C) and was heated to 95 °C. The reaction mixture was allowed to cool to room temperature and the resulting precipitate was collected and dried under vacuum to obtain 55. Yield 61%. ¹H NMR (300 MHz, DMSO-*d*₆): δ = 3.17 (dd, 1H, *J* = 14.1 Hz, *J* = 8.9 Hz), 3.37 (dd, 1H, *J* = 14.1 Hz, *J* = 4.6 Hz), 5.04 (dd, 1H, *J* = 8.9 Hz, *J* = 4.6 Hz), 7.27 (m, 5H), 13.2 (bs, 1H). ¹³C NMR (75 MHz, acetone-*d*₆): δ = 27.8, 46.9, 118.4, 119.8, 120.5, 127.9, 169.2, 194.6. HRMS (ESI, [M - H]⁻) calcd (C₁₀H₈NOS₂) 222.0126; found 222.0061.

5-(3,4-Dihydroxybenzyl)-2-thioxoimidazolidin-4-one (56). 56 was synthesized according to procedures A and B. Yield 15%. ¹H NMR (300 MHz, acetone-*d*₆): δ = 2.82 (dd, 1H, *J* = 14.1 Hz, *J* = 6.9 Hz), 3.04 (dd, 1H, *J* = 14.1 Hz, *J* = 6.8 Hz), 4.38 (dt, 1H, *J* = 5.7 Hz, *J* = 1.2 Hz), 6.53 (dd, 1H, *J* = 8.1 Hz, *J* = 1.9 Hz), 6.68 (d, 1H, *J* = 5.5 Hz), 6.60 (d, 1H, *J* = 8.0 Hz), 8.81 (bs, 1H), 10.3 (bs, 1H). ¹³C NMR (75 MHz, DMSO-*d*₆): δ = 29.7, 60.9, 125.3, 126.7, 126.9, 135.9, 175.3, 182.6. HRMS (ESI, [M - H]⁻) calcd (C₁₀H₉N₂O₃S) 237.0412; found 237.0334.

5-(3,4-Dihydroxybenzyl)imidazolidine-2,4-dione (57). See procedure for 53. Yield 81%. ¹H NMR (300 MHz, DMSO-*d*₆): δ = 2.73 (d, 2H, *J* = 4.3 Hz), 4.19 (t, 1H, *J* = 4.3 Hz), 6.42 (dd, 1H, *J* = 8.0 Hz, *J* = 2.1 Hz), 6.65 (d, 1H, *J* = 2.0 Hz), 6.60 (d, 1H, *J* = 8.0 Hz), 7.81 (bs, 1H), 10.4 (bs, 1H). ¹³C NMR (75 MHz, DMSO-*d*₆): δ = 35.7, 58.6, 120.4, 126.1, 143.8, 144.6, 157.1, 175.2. HRMS (ESI, [M - H]⁻) calcd (C₁₀H₉N₂O₄) 221.0641; found 221.0575.

5-(Thiophen-2-ylmethyl)-2-thioxoimidazolidin-4-one (58). 58 was synthesized according to procedures A and B. Yield 40%. ¹H NMR (300 MHz, DMSO-*d*₆): δ = 3.21 (ddd, 2H, *J* = 15.3 Hz, *J* = 10.5 Hz, *J* = 4.3 Hz), 4.54 (dt, 1H, *J* = 4.6 Hz, *J* = 1.1 Hz), 6.85 (dd, 1H, *J* = 3.4 Hz, *J* = 0.9 Hz), 6.94 (dd, 1H, *J* = 5.1 Hz, *J* = 3.4 Hz), 7.37 (dd, 1H, *J* = 5.1 Hz, *J* = 1.2 Hz), 10.1 (bs, 1H), 11.5 (bs, 1H). ¹³C NMR (75 MHz, DMSO-*d*₆): δ = 29.7, 60.9, 125.3, 126.7, 126.9, 135.9, 175.3, 182.6. HRMS (ESI, [M - H]⁻) calcd (C₈H₇N₂O₂S) 211.0078; found 211.0005.

5-(Thiophen-2-ylmethyl)imidazolidine-2,4-dione (59). See procedure for 53. Yield 62%. ¹H NMR (300 MHz, DMSO-*d*₆): δ =

3.15 (ddd, 2H, $J = 15.1$ Hz, $J = 11.5$ Hz, $J = 4.6$ Hz), 4.31 (dt, 1H, $J = 4.5$ Hz, $J = 1.2$ Hz), 6.86 (dd, 1H, $J = 3.3$ Hz, $J = 0.9$ Hz), 6.95 (dd, 1H, $J = 5.1$ Hz, $J = 3.4$ Hz), 7.36 (dd, 1H, $J = 5.1$ Hz, $J = 1.2$ Hz), 7.96 (bs, 1H), 10.5 (bs, 1H). ^{13}C NMR (75 MHz, DMSO- d_6): $\delta = 30.5$, 57.9, 125.0, 126.7, 126.9, 136.6, 157.2, 174.8. HRMS (ESI, $[\text{M} - \text{H}]^-$) calcd ($\text{C}_8\text{H}_7\text{N}_2\text{O}_2\text{S}$) 195.0306; found 198.0224.

(S)-5-((1*H*-Indol-3-yl)methyl)imidazolidine-2,4-dione (60). See procedure for **53**. Yield 79%. ^1H NMR (300 MHz, DMSO- d_6): $\delta = 3.06$ (d, 2H, $J = 4.8$ Hz), 4.30 (t, 1H, $J = 5.0$ Hz), 6.96 (t, 1H, $J = 7.9$ Hz), 7.05 (t, 1H, $J = 8.0$ Hz), 7.11 (d, 1H, $J = 2.3$ Hz), 7.31 (d, 1H, $J = 8.0$ Hz), 7.54 (d, 1H, $J = 7.8$ Hz), 7.88 (bs, 1H), 10.4 (bs, 1H), 10.9 (bs, 1H). ^{13}C NMR (75 MHz, DMSO- d_6): $\delta = 26.5$, 58.3, 107.9, 111.2, 118.3, 118.5, 120.8, 124.1, 127.5, 135.8, 157.3, 175.7. HRMS (ESI, $[\text{M} - \text{H}]^-$) calcd ($\text{C}_{12}\text{H}_{10}\text{N}_3\text{O}_2$) 228.0851; found 228.0778.

■ ASSOCIATED CONTENT

Supporting Information

Details on chemistry and analytical data; a tabular overview of binding modes of FMMH derivatives in protein–ligand complexes. This material is available free of charge via the Internet at <http://pubs.acs.org>.

■ AUTHOR INFORMATION

Corresponding Author

*Phone: ++49-6221-554875. E-mail: c.klein@uni-heidelberg.de.

■ ACKNOWLEDGMENTS

We thank Therese Scholz, Aline Marschner, and Michael Wacker for performing MurA and MetAP assays, Heiko Rudy for measuring the EI and ESI high resolution spectra, and Christian Frank for the synthesis of **45–51** during the course of a medicinal chemistry internship. We also thank Prof. G. Fricker for providing access to the dynamic light scattering instrument and Dr. Frank Rominger for performing the small-molecule X-ray-analysis.

■ ABBREVIATIONS USED

FMMH, five-membered multiheterocycle; DLS, dynamic light scattering; DFT, density functional theory; CPMD, Car–Parrinello molecular dynamics; MetAP, methionine aminopeptidase; NS2B-NS3, protease from Dengue virus; MurA, UDP-*N*-acetylglucosamine enolpyruvyl transferase; SAR, structure–activity relationship

■ REFERENCES

- (1) Baell, J. B.; Holloway, G. A. New Substructure Filters for Removal of Pan Assay Interference Compounds (PAINS) from Screening Libraries and for Their Exclusion in Bioassays. *J. Med. Chem.* **2010**, *53*, 2719–2740.
- (2) Tomicic, T.; Masic, L. P. Rhodanine as a Privileged Scaffold in Drug Discovery. *Curr. Med. Chem.* **2009**, *16*, 1596–1629.
- (3) Tomicic, T.; Zidar, N.; Kovac, A.; Turk, S.; Simcic, M.; Blanot, D.; Mueller-Premru, M.; Filipic, M.; Grdadolnik, S. G.; Zega, A.; Anderlueh, M.; Gobec, S.; Kikelj, D.; Masic, L. P. 5-Benzylidenethiazolidin-4-ones as Multitarget Inhibitors of Bacterial Mur Ligases. *ChemMedChem* **2010**, *5*, 286–295.
- (4) Bachelier, A.; Mayer, R.; Klein, C. D. Sesquiterpene Lactones Are Potent and Irreversible Inhibitors of the Antibacterial Target Enzyme MurA. *Bioorg. Med. Chem. Lett.* **2006**, *16*, 5605–5609.
- (5) Steuer, C.; Heinonen, K. H.; Kattner, L.; Klein, C. D. Optimization of Assay Conditions for Dengue Virus Protease: Effect of Various Polyols and Nonionic Detergents. *J. Biomol. Screening* **2009**, *14*, 1102–1108.
- (6) McGovern, S. L.; Caselli, E.; Grigorieff, N.; Shoichet, B. K. A Common Mechanism Underlying Promiscuous Inhibitors from Virtual and High-Throughput Screening. *J. Med. Chem.* **2002**, *45*, 1712–1722.
- (7) Mendgen, T.; Scholz, T.; Klein, C. D. Structure–Activity Relationships of Tulipalines, Tuliposides, and Related Compounds as Inhibitors of MurA. *Bioorg. Med. Chem. Lett.* **2010**, *20*, 5757–5762.
- (8) Steuer, C.; Gege, C.; Fischl, W.; Heinonen, K. H.; Bartenschlager, R.; Klein, C. D. Synthesis and Biological Evaluation of α -Ketoamides As Inhibitors of the Dengue Virus Protease with Antiviral Activity in Cell-Culture. *Bioorg. Med. Chem.* **2011**, *19*, 4067–4074.
- (9) Ma, L. A.; Xie, C. F.; Ma, Y. H.; Liu, J. A.; Xiang, M. L.; Ye, X.; Zheng, H.; Chen, Z. Z.; Xu, Q. Y.; Chen, T.; Chen, J. Y.; Yang, J. C.; Qiu, N.; Wang, G. C.; Liang, X. L.; Peng, A. H.; Yang, S. Y.; Wei, Y. Q.; Chen, L. J. Synthesis and Biological Evaluation of Novel 5-Benzylidenethiazolidine-2,4-dione Derivatives for the Treatment of Inflammatory Diseases. *J. Med. Chem.* **2011**, *54*, 2060–2068.
- (10) Radi, M.; Botta, L.; Casaluce, G.; Bernardini, M.; Botta, M. Practical One-Pot Two-Step Protocol for the Microwave-Assisted Synthesis of Highly Functionalized Rhodanine Derivatives. *J. Comb. Chem.* **2010**, *12*, 200–205.
- (11) Zuliani, V.; Carmi, C.; Rivara, M.; Fantini, M.; Lodola, A.; Vacondio, F.; Bordini, F.; Plazzi, P. V.; Cavazzoni, A.; Galetti, M.; Alfieri, R. R.; Petronini, P. G.; Mora, M. 5-Benzylidene-hydantoins: Synthesis and Antiproliferative Activity on A549 Lung Cancer Cell Line. *Eur. J. Med. Chem.* **2009**, *44*, 3471–3479.
- (12) Anderlueh, M.; Jukic, M.; Petric, R. Three-Component One-Pot Synthetic Route to 2-Amino-5-alkylidene-thiazol-4-ones. *Tetrahedron* **2009**, *65*, 344–350.
- (13) Villain-Guillot, P.; Gualtieri, M.; Bastide, L.; Roquet, F.; Martinez, J.; Amblard, M.; Pugniere, M.; Leonetti, J. P. Structure–Activity Relationships of Phenyl-furanyl-rhodanines as Inhibitors of RNA Polymerase with Antibacterial Activity on Biofilms. *J. Med. Chem.* **2007**, *50*, 4195–4204.
- (14) Lamiri, M.; Bougrin, K.; Daou, B.; Soufiaoui, M.; Nicolas, E.; Giralt, E. Microwave-Assisted Solvent-Free Regiospecific Synthesis of 5-Alkylidene and 5-Arylidenehydantoins. *Synth. Commun.* **2006**, *36*, 1575–1584.
- (15) Joshi, M.; Vargas, C.; Boisguerin, P.; Diehl, A.; Krause, G.; Schmieder, P.; Moelling, K.; Hagen, V.; Schade, M.; Oschkinat, H. Discovery of Low-Molecular-Weight Ligands for the AF6 PDZ Domain. *Angew. Chem., Int. Ed.* **2006**, *45*, 3790–3795.
- (16) Unangst, P. C.; Connor, D. T.; Cetenko, W. A.; Sorenson, R. J.; Kostlan, C. R.; Sircar, J. C.; Wright, C. D.; Schrier, D. J.; Dyer, R. D. Synthesis and Biological Evaluation of 5-[[3,5-Bis(1,1-dimethylethyl)-4-hydroxyphenyl]methylene]oxazoles, -thiazoles, and -imidazoles: Novel Dual 5-Lipoxygenase and Cyclooxygenase Inhibitors with Antiinflammatory Activity. *J. Med. Chem.* **1994**, *37*, 322–328.
- (17) Xia, Z.; Knaak, C.; Ma, J.; Beharry, Z. M.; McInnes, C.; Wang, W.; Kraft, A. S.; Smith, C. D. Synthesis and Evaluation of Novel Inhibitors of Pim-1 and Pim-2 Protein Kinases. *J. Med. Chem.* **2009**, *52*, 74–86.
- (18) Bruno, G.; Costantino, L.; Curinga, C.; Maccari, R.; Monforte, F.; Nicolo, F.; Ottana, R.; Vigorita, M. G. Synthesis and Aldose Reductase Inhibitory Activity of 5-Arylidene-2,4-thiazolidinediones. *Bioorg. Med. Chem.* **2002**, *10*, 1077–1084.
- (19) Gregg, B. T.; Golden, K. C.; Quinn, J. F.; Tymoshenko, D. O.; Earley, W. G.; Maynard, D. A.; Razzano, D. A.; Rennells, W. M.; Butcher, J. Expedient Lewis Acid Catalyzed Synthesis of a 3-Substituted 5-Arylidene-1-methyl-2-thiohydantoin Library. *J. Comb. Chem.* **2007**, *9*, 1036–1040.
- (20) Wang, Z. D.; Sheikh, S. O.; Zhang, Y. L. A Simple Synthesis of 2-Thiohydantoins. *Molecules* **2006**, *11*, 739–750.
- (21) Reyes, S.; Burgess, K. On Formation of Thiohydantoins from Amino Acids under Acylation Conditions. *J. Org. Chem.* **2006**, *71*, 2507–2509.
- (22) Ooms, F.; Wouters, J.; Oscari, O.; Happaerts, T.; Bouchard, G.; Carrupt, P. A.; Testa, B.; Lambert, D. M. Exploration of the Pharmacophore of 3-Alkyl-5-arylimidazolidinediones as New CB1 Cannabinoid Receptor Ligands and Potential Antagonists: Synthesis,

Lipophilicity, Affinity, and Molecular Modeling. *J. Med. Chem.* **2002**, *45*, 1748–1756.

(23) Mohler, D. L.; Shen, G.; Dotse, A. K. Solution- and Solid-Phase Synthesis of Peptide-Substituted Thiazolidinediones as Potential PPAR Ligands. *Bioorg. Med. Chem. Lett.* **2000**, *10*, 2239–2242.

(24) Liu, W.; Liu, K.; Wood, H. B.; McCann, M. E.; Doebber, T. W.; Chang, C. H.; Akiyama, T. E.; Einstein, M.; Berger, J. P.; Meinke, P. T. Discovery of a Peroxisome Proliferator Activated Receptor gamma (PPAR gamma) Modulator with Balanced PPAR alpha Activity for the Treatment of Type 2 Diabetes and Dyslipidemia. *J. Med. Chem.* **2009**, *52*, 4443–4453.

(25) Suarez, A.; Lopez, F.; Compagnone, R. S. Stereospecific Synthesis of the Lignans: 2-S-(3,4-Dimethoxybenzyl)-3-R-(3,4,5-trimethoxybenzyl)butyrolactone and Its Positional Isomeric Lactone. *Synth. Commun.* **1993**, *23*, 1991–2001.

(26) Campbell, N.; McKail, J. E. 248. The Preparation of the Halogenophenylacetic Acids. *J. Chem. Soc.* **1948**, 1251–1255.

(27) Lanzetta, P. A.; Alvarez, L. J.; Reinach, P. S.; Candia, O. A. An Improved Assay for Nanomole Amounts of Inorganic Phosphate. *Anal. Biochem.* **1979**, *100*, 95–7.

(28) Altmeyer, M. A.; Marschner, A.; Schiffmann, R.; Klein, C. D. Subtype-Selectivity of Metal-Dependent Methionine Aminopeptidase Inhibitors. *Bioorg. Med. Chem. Lett.* **2010**, *20*, 4038–4044.

(29) Schiffmann, R.; Neugebauer, A.; Klein, C. D. Metal-Mediated Inhibition of *Escherichia coli* Methionine Aminopeptidase: Structure–Activity Relationships and Development of a Novel Scoring Function for Metal–Ligand Interactions. *J. Med. Chem.* **2006**, *49*, 511–522.

(30) Powers, J. P.; Piper, D. E.; Li, Y.; Mayorga, V.; Anzola, J.; Chen, J. M.; Jaen, J. C.; Lee, G.; Liu, J. Q.; Peterson, M. G.; Tonn, G. R.; Ye, Q. P.; Walker, N. P. C.; Wang, Z. L. SAR and Mode of Action of Novel Non-Nucleoside Inhibitors of Hepatitis C NSSb RNA Polymerase. *J. Med. Chem.* **2006**, *49*, 1034–1046.

(31) Feng, B. Y.; Shelat, A.; Doman, T. N.; Guy, R. K.; Shoichet, B. K. High-Throughput Assays for Promiscuous Inhibitors. *Nat. Chem. Biol.* **2005**, *1*, 146–148.

(32) Ryan, A. J.; Gray, N. M.; Lowe, P. N.; Chung, C. W. Effect of Detergent on “Promiscuous” Inhibitors. *J. Med. Chem.* **2003**, *46*, 3448–3451.

(33) CPMD; IBM Corp., 1990–2011; MPI fuer Festkoerperforschung Stuttgart, 1997–2001.

(34) Varetto, U. *Molekel*, version 5.4.0.8; Swiss National Supercomputing Centre: Manno, Switzerland.

(35) Allen, F. H.; Wood, P. A.; Pidcock, E. Interaction Geometries and Energies of Hydrogen Bonds to C=O and C=S Acceptors: A Comparative Study. *Acta Crystallogr., Sect. B: Struct. Sci.* **2008**, *64*, 491–496.

(36) Allen, F. H.; Bird, C. M.; Rowland, R. S.; Raithby, P. R. Resonance-Induced Hydrogen Bonding at Sulfur Acceptors in R1R2C=C and R1CS2 Systems. *Acta Crystallogr., Sect. B: Struct. Sci.* **1997**, *53*, 680–695.

(37) Custelcean, R. Crystal Engineering with Urea and Thiourea Hydrogen-Bonding Groups. *Chem. Commun.* **2008**, 295–307.

(38) Diamond, S. L. Thrombin 1536 HTS, Assay ID 1046. http://pubchem.ncbi.nlm.nih.gov/assay/assay.cgi?aid=1046&loc=ea_ras (accessed Apr 2, 2010).

(39) Berman, H. M.; Westbrook, J.; Feng, Z.; Gilliland, G.; Bhat, T. N.; Weissig, H.; Shindyalov, I. N.; Bourne, P. E. The Protein Data Bank. *Nucleic Acids Res.* **2000**, *28*, 235–242.

(40) Yesudas, J. P.; Sayyed, F. B.; Suresh, C. H. Analysis of Structural Water and CH $\cdots\pi$ Interactions in HIV-1 Protease and PTP1B Complexes Using a Hydrogen Bond Prediction Tool, HBPredicT. *J. Mol. Model.* **2011**, *17*, 401–413.

(41) DeLano, W. L. *The PyMOL Molecular Graphics System*; DeLano Scientific: San Carlos, CA, U.S., 2002.

(42) Car, R.; Parrinello, M. Unified Approach for Molecular Dynamics and Density-Functional Theory. *Phys. Rev. Lett.* **1985**, *55*, 2471.

(43) Lee, C.; Yang, W.; Parr, R. G. Development of the Colle–Salvetti Correlation-Energy Formula into a Functional of the Electron Density. *Phys. Rev. B: Condens. Matter* **1988**, *37*, 785.

(44) Becke, A. D. Density-Functional Exchange-Energy Approximation with Correct Asymptotic Behavior. *Phys. Rev. A: At, Mol, Opt. Phys.* **1988**, *38*, 3098.